

This article was downloaded by:

On: 26 January 2011

Access details: *Access Details: Free Access*

Publisher *Taylor & Francis*

Informa Ltd Registered in England and Wales Registered Number: 1072954 Registered office: Mortimer House, 37-41 Mortimer Street, London W1T 3JH, UK



Liquid Crystals

Publication details, including instructions for authors and subscription information:

<http://www.informaworld.com/smpp/title~content=t713926090>

New chiral thiobenzoate series with antiferroelectric mesophases

H. T. Nguyen^a; J. C. Rouillon^a; P. Cluzeau^a; G. Sigaud^a; C. Destrade^a; N. Isaert^b

^a Centre de Recherche Paul Pascal/C.N.R.S., Université de Bordeaux I, Pessac, France ^b Laboratoire de Dynamique et Structure des Matériaux Moléculaires, Université de Lille 1, Villeneuve d'Ascq Cedex, France

To cite this Article Nguyen, H. T. , Rouillon, J. C. , Cluzeau, P. , Sigaud, G. , Destrade, C. and Isaert, N.(1994) 'New chiral thiobenzoate series with antiferroelectric mesophases', *Liquid Crystals*, 17: 4, 571 — 583

To link to this Article: DOI: 10.1080/02678299408036741

URL: <http://dx.doi.org/10.1080/02678299408036741>

PLEASE SCROLL DOWN FOR ARTICLE

Full terms and conditions of use: <http://www.informaworld.com/terms-and-conditions-of-access.pdf>

This article may be used for research, teaching and private study purposes. Any substantial or systematic reproduction, re-distribution, re-selling, loan or sub-licensing, systematic supply or distribution in any form to anyone is expressly forbidden.

The publisher does not give any warranty express or implied or make any representation that the contents will be complete or accurate or up to date. The accuracy of any instructions, formulae and drug doses should be independently verified with primary sources. The publisher shall not be liable for any loss, actions, claims, proceedings, demand or costs or damages whatsoever or howsoever caused arising directly or indirectly in connection with or arising out of the use of this material.

New chiral thiobenzoate series with antiferroelectric mesophases

by H. T. NGUYEN*†, J. C. ROUILLON†, P. CLUZEAU†,
G. SIGAUD†, C. DESTRADE† and N. ISAERT‡

† Centre de Recherche Paul Pascal/C.N.R.S., Université de Bordeaux I,
Avenue A. Schweitzer, F-33600 Pessac, France

‡ Laboratoire de Dynamique et Structure des Matériaux Moléculaires,
Université de Lille 1, F-59655 Villeneuve d'Ascq Cedex, France

(Received 29 November 1993; accepted 2 March 1994)

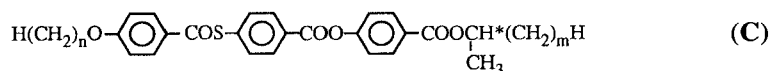
A new series of chiral homologous thiobenzoates with non-chiral end chains ranging from heptyloxy to octadecyloxy has been synthesized and characterized. The mesomorphic properties have been analysed by optical microscopy on pure compounds and mixtures, DSC, and electro-optical and pitch measurements. They display a very rich polymesomorphism including S_A , S_{CA}^* , S_C^* , S_{CFI}^* , S_{CA}^* phases with reference to the compound MHPOBC through miscibility tests. Peculiarly noticeable are: (i) two S_{CFI}^* phases sandwiched between S_C^* and S_{CA}^* phases in some compounds; (ii) full miscibility between the S_{CA}^* phase and the S_C^* phase of the racemic reference compound MHTAC which leads us to question whether the S_{CA}^* or S_C^* symbol should be used to designate the antiferroelectric smectic C^* phase; (iii) odd-even cancellation of the S_{CA}^* phase in relation to both the chiral chain and the alkyloxy chain; (iv) a reentrant sequence, $C S_C S_{CA} S_C S_A I$, in a pure compound assessed by a phase diagram. The electro-optical measurements were carried out with the classical SSFLC geometry. The field threshold is determined for each titled mesophase. One can note: (i) a low threshold whatever the phase; (ii) a first plateau at $0.4 \text{ V } \mu\text{m}^{-1}$ and a saturation at $1 \text{ V } \mu\text{m}^{-1}$ in the S_{CFI}^* phase; (iii) strong pretransitional variations of the pitch at the $S_{CA}^*-S_{CFI}^*$ and $S_{CFI}^*-S_C^*$ transitions.

1. Introduction

Chiral ferroelectric mesogens have been paid much attention especially during the last four years as materials for display application [1-4]. A side issue of this wide search has been the description of numerous complex structures combining chirality, smectic layers and dipole order [5-10]. This paper presents a detailed analysis of a new chiral series derived from 4-mercaptobenzoic acid.

2. Materials

The compounds studied have the following general formula:



where $n = 7-12, 16, 18$ and $m = 4-8$.

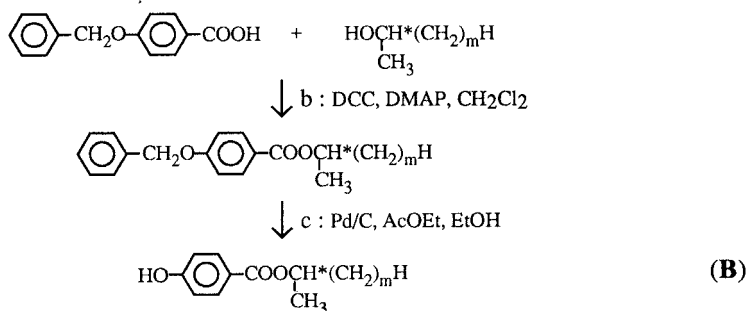
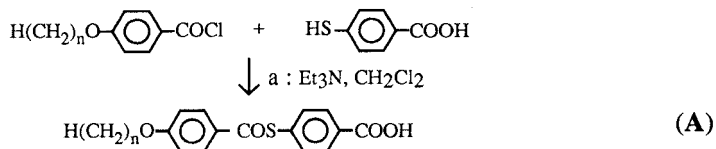
* Author for correspondence.

Table 1. Transition temperatures ($^{\circ}\text{C}$) and enthalpies (kJ mol^{-1}) for the chiral compounds with $m = 6$.

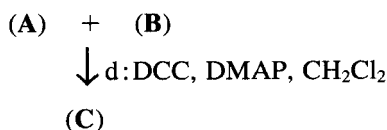
n	m	C	S_{C}^{\ddagger}	$S_{\text{CFI}}^{\ddagger}$	$S_{\text{CFI2}}^{\ddagger}$	S_{C}^{\ddagger}	S_{A}^{\ddagger}	S_{C}^{\ddagger}	S_{A}^{\ddagger}	I
7	6	•	—	—	—	—	—	—	—	•
		83.7								161.7
		28.6								6.0
8	6	•	—	—	—	•	(75)	•	(83)	•
		86.3					0.002		0.003	159.2
		36.4								6.2
9	6	•	(91)	•	•	109.2	•	•	115.5	•
		101.3	0.003			0.004			0.06	155.4
		40.1		†						6.1
10	6	•	112	•	•	119.2	•	•	123.6	•
		109.7	0.004			0.003			0.06	152.6
		45.5		0.002						6.2
11	6	•	101	•	•	111	•	•	128	•
		95.5	0.003			0.008			0.1	149
		49		†						5.8
12	6	•	111	•	•	115	•	•	130	•
		82.4	0.004			0.013			0.27	146
		27.4		†						5.9
16	6	•	73	—	•	88	•	•	—	•
		67	0.004			0.003				134
		41								5.5
18	6	•	—	—	—	•	•	•	•	•
		62				124				132
		41				0.26				5.3

† Transition enthalpy $\leq 1 \text{ J mol}^{-1}$.

The synthetic route is briefly summarized below:



Finally:



Following the same scheme, a few racemic compounds have also been prepared with $n = 10-11$ and $m = 4-8$.

3. Mesomorphic properties

The phase behaviour of the series of chiral compounds is summarized in table 1 and figure 1. The compounds are smectic A (S_A) over the entire series. The clearing temperature decreases regularly with no odd-even effect. The smectic S_C^* precedes the helical smectics from $n = 8$ to $n = 12$. As usual its temperature range is limited. The ferroelectric smectic C^* phase (S_C^*) appears at $n = 10$ and becomes dominant over all

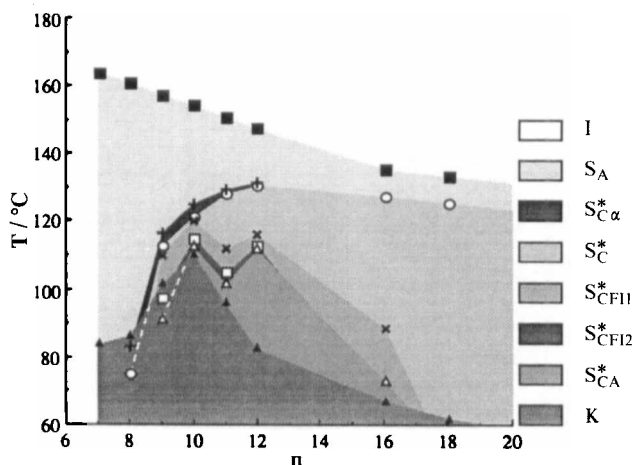


Figure 1. Phase behaviour of the chiral compounds as a function of alkoxy chain length.

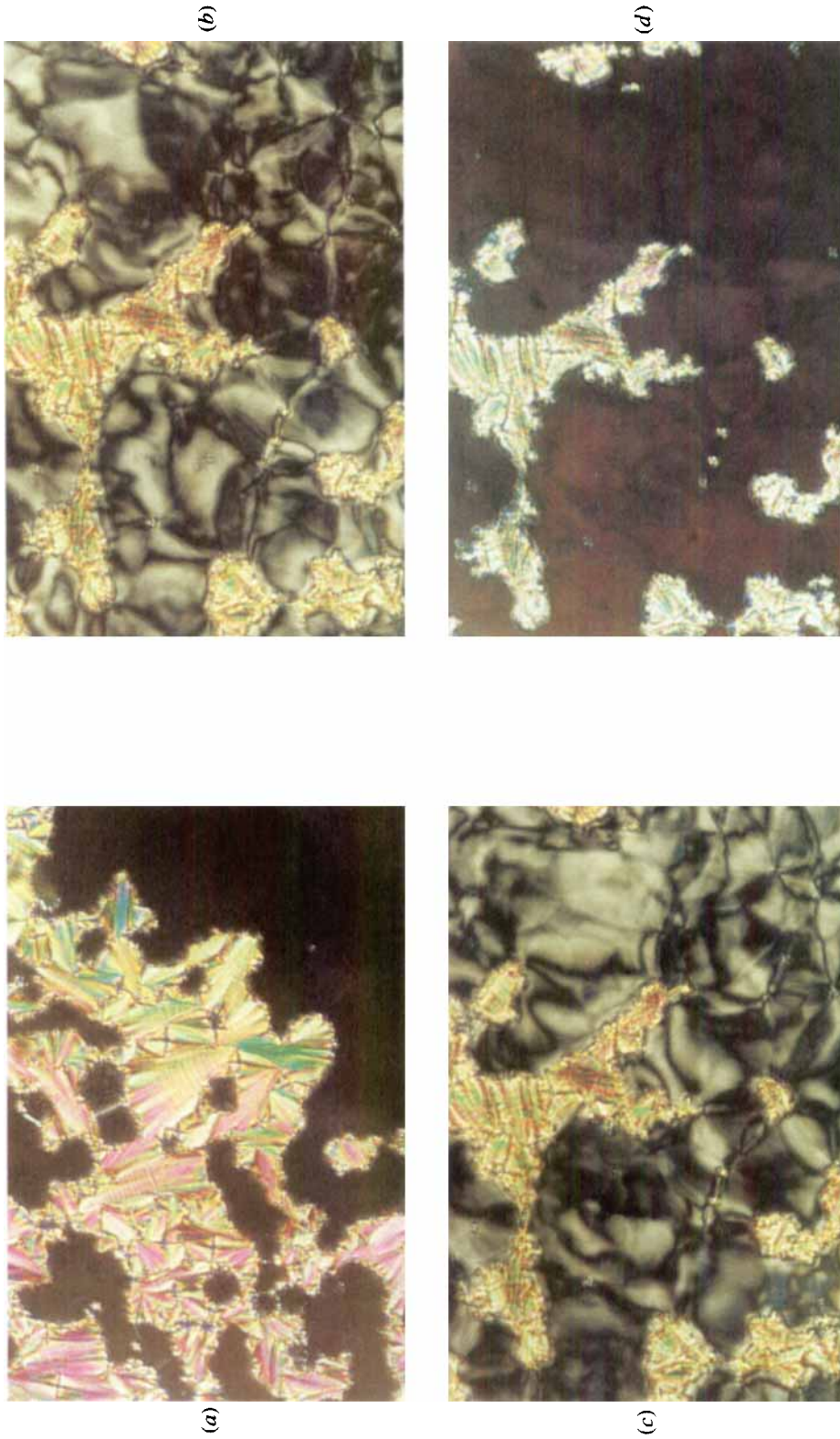


Figure 2. Sequence of microscopic textures obtained upon cooling a sample of thiobenzate with $n = 11$ and $m = 6$: (a) 120°C (S_{FI}^*); (b) 106°C (S_{FI2}^*); (c) 101°C (S_{FI}^*); (d) 97°C (S_A^*).

other phases for longer alkoxy chains. The antiferroelectric smectic C* phase (S_{CA}^*) is detected from $n = 9$ to $n = 16$. The temperature range also decreases with the chain length.

No direct change from S_C^* to S_{CA}^* could be observed in this series of pure chiral compounds. When simultaneously obtained, the two phases are always separated by one or two intermediate ferroelectric phases (S_{CFi}^*).

As an example of the microscopic characterization, figure 2 shows the modification of the texture in a sample of the undecyloxy derivative on passing from S_C^* (figure 2 (a)) to S_{CA}^* (figure 2 (d)) via the two intermediate phases (figures 2 (b) and (c)), supposedly of the same S_{CFi}^* type (see further discussion). The above assignment of the different smectic phases relies mainly on the miscibility diagram between this undecyloxy derivative and the well-known compound MHPOBC shown in figure 3. In this way we have been able to assess the isomorphism for all phases but one. This additional

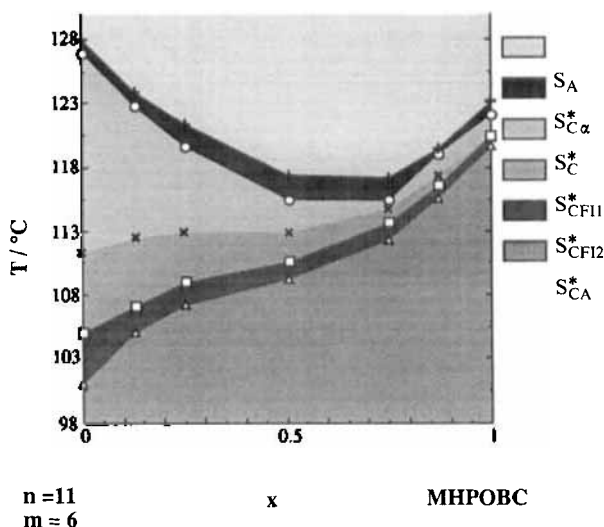


Figure 3. Isobaric binary phase diagram showing the isomorphy of the phases of the thiobenzoate with $n = 11$ and $m = 6$ with MHPOBC:

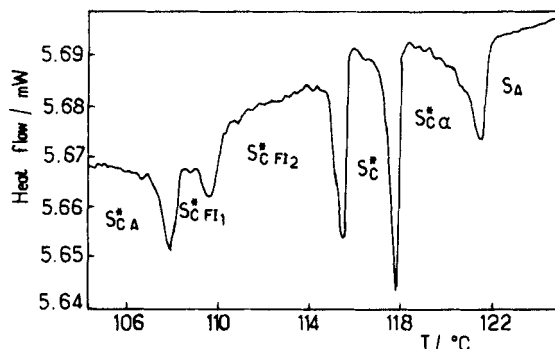
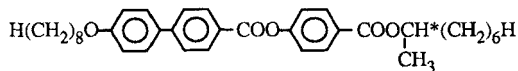


Figure 4. DSC thermogram for the chiral decyloxy derivative.

Table 2. Transition temperatures (°C) for racemic compounds.

<i>n</i>	<i>m</i>	C	S _C	S _{C_A}	S _C	S _A	I
10	4	● 96	—	● 122	● 123.5	● 160	●
11	4	● 92	—	● 121	● 130	● 157	●
10	5	● 90	—	—	● 123.5	● 155	●
11	5	● 87	—	—	● 130	● 153	●
11	6	● 78	—	—	● 126	● 148	●
12	6	● 61	● 65	● 103	● 128	● 144	●
13	6	● 59	—	—	● 130.5	● 143	●
10	7	● 84	—	—	● 119	● 146	●
11	7	● 76	—	—	● 125	● 145	●
10	8	● 80	—	● 91	● 117	● 144	●
11	8	● 72	—	—	● 122	● 141	●

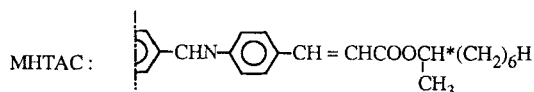
Table 3. Transition temperatures (°C) for the chiral compounds with *m* = 5 or 6.

<i>n</i>	<i>m</i>	C	S _{C_A} [*]	S _{C_{FI1}} [*]	S _{C_{FI2}} [*]	S _C [*]	S _{C_z} [*]	S _A	I
10	5	● 107	—	—	—	● 119	—	● 153	●
11	5	● 104	—	—	—	● 129	—	● 151	●
10	6†	● 106	● 112	● 114	● 119.2	● 120	● 122	● 150	●
11	6†	● 95.5	● 101	● 104.5	● 111	● 125	● 126	● 147	●

† From table 1.

mesophase is clearly detected by optical observations and DSC (see figure 4) in several compounds of the series. Our suggestion that it could be another ferrielectric smectic C* is based on the pitch measurements described later.

At this point it is worth recalling that a previous study of miscibility carried out by Heppke *et al.* [11], using MHPOBC (see caption to figure 3), with MHTAC, shown below, has shown that the S_{C_A}^{*} phase of the former is isomorphous with the S_C^{*} phase reported in the latter by Levelut *et al.* [12–14]. We have confirmed these observations with our compounds. One of the symbols then appears redundant.



The racemic compounds in table 2 and the chiral compounds in table 3 help us to discuss in a more detailed manner the behaviour of these closely related phases with respect to chain lengths. The phenomenon which is especially spectacular in these tables is the odd–even cancellation of the S_{C_A}^{*} or S_{C_A} phases [15]. The effect with *m* appears most dramatic: neither a S_{C_A} nor a S_{C_A}^{*} is observed with odd values. Although the S_{C_A} phase is also absent for odd values of *n*, this odd–even influence of *n* appears milder on the S_{C_A}^{*} phases of the chiral compounds (see table 1). An even–even combination of chains is obviously required to obtain the S_{C_A} phase, but not for the S_{C_A}^{*} one. The crucial role of the parity of the chiral chain (*m*) shows up for all the other helical structures except the S_C^{*} phase (see table 3). Note finally a reentrant smectic C phase in the pure racemic compound (*n* = 12, *m* = 6) in table 2. This phenomenon was previously mentioned by Hamelin *et al.* [16], and Heppke *et al.* [11], in the MHTAC series.

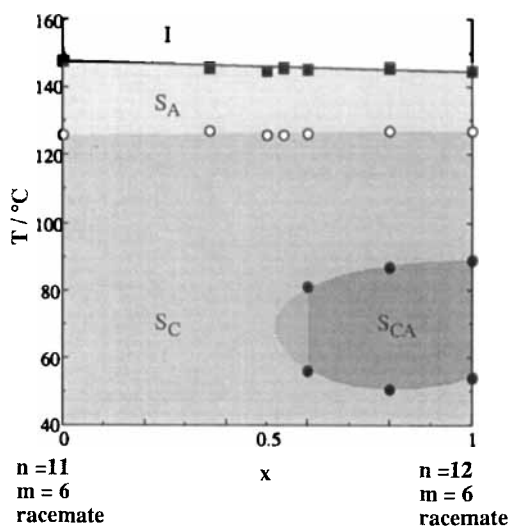


Figure 5. Isobaric phase diagram between the two successive homologous racemates with $n = 11$ (left) and $n = 12$ (right).

4. Miscibility studies

An additional study of phase diagrams has been conducted involving the racemic compounds in table 3. We first checked the reentrant character of the S_C phase of the dodecyl racemate and studied its binary diagram with the undecyloxy homologue. This behaviour is clearly shown in figure 5 in which the S_C phase surrounds the S_{C_A} domain. It must be mentioned that hysteresis plays an important role at the transitions among S_C , S_{C_A} and $S_{C_{re}}$ phases. (All temperature measurements for the phase diagrams are reported upon cooling.) Moreover the textural differences between the S_{C_A} and S_C phases are far less obvious than those between a nematic and a smectic A phase in cases of nematic reentrance. For this reason the termination of the S_{C_A} domain is difficult to locate precisely and could only be extrapolated. Nevertheless the S_{C_A} phase is undoubtedly absent for a molar fraction of less than 0.5 for the undecyloxy compound.

Then we used this technique to check the miscibility between the chiral $\{(R) \text{ or } (S)\}$ dodecyloxy enantiomer and its racemate. The diagram in figure 6 shows total miscibility between the two S_A phases, the high temperature S_C and the S_C^* phases and the S_{C_A} and the $S_{C_A}^*$ phases. The transition between the $S_{C_A}^*$ phase and low temperature reentrant S_C —alternatively S_C^* —progressively drops toward crystallization. On the other side the $S_{C_x}^*$ and $S_{C_{FI(1+2)}}^*$ phases soon disappear with decreasing chirality (molar fraction of the racemic compound > 0.3). At lower enantiomer content of the mixture, DSC and optical microscopic observations agree with a direct transition between S_C^* and $S_{C_A}^*$ phases. Although previously reported in pure chiral materials [17], this behaviour is only detected in our work in these mixtures where the optical purity is lowered.

Finally, figure 7 shows the miscibility of the S_C^* and S_C phases of the undecyloxy derivative and its racemic analogue, respectively. The extension of the $S_{C_{FI(1+2)}}^*$ phases above the $S_{C_A}^*$ phase is notable in this system: it makes it impossible to reach a direct $S_C^* - S_{C_A}^*$ transition as previously mentioned by Hamelin [16]. Note in this case too the rapid expulsion of the $S_{C_x}^*$ phase.

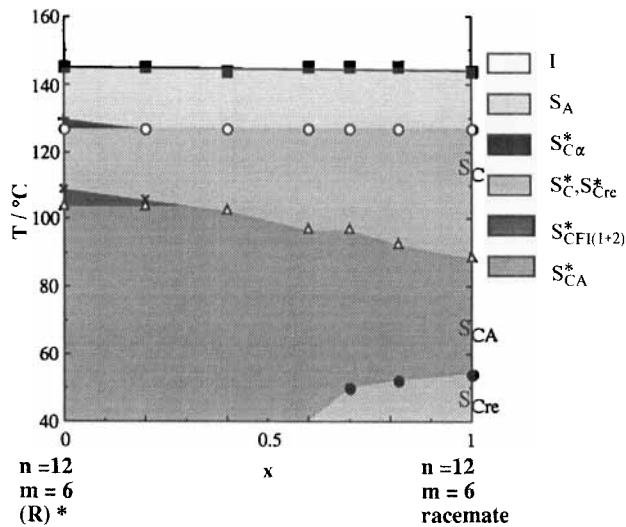


Figure 6. Isobaric phase diagram between the $n=12$, $m=6$ enantiomer (left) and its homologous racemate (right). S_{Cre} for reentrant smectic C.

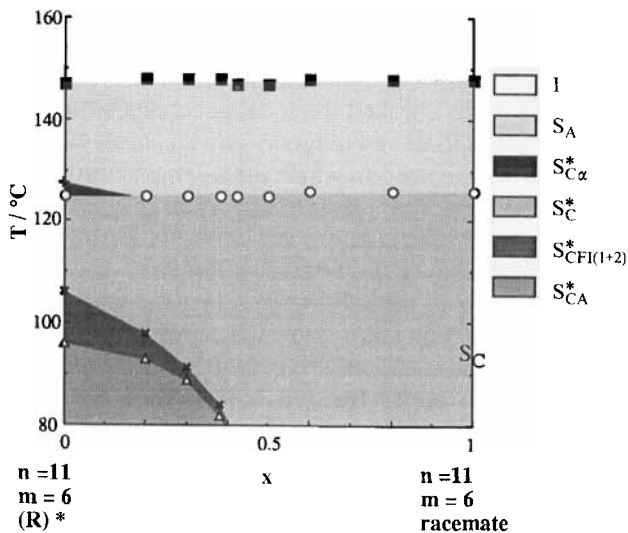


Figure 7. Isobaric phase diagram between the $n=11$, $m=6$ enantiomer (left) and its homologous racemate (right).

5. Electro-optic properties

These have been investigated using the undecyloxy compound. The material was confined between two ITO coated glass slides; the active area was 0.25 cm^2 . To achieve a planar alignment the glass surfaces were coated with a polyimide layer which was rubbed unidirectionally. The thickness of the cell was $7.5 \mu\text{m}$ (obtained using fibre glass spacers). A good planar orientation was achieved by slow cooling through the isotropic to S_A phase transition ($0.1^\circ\text{C min}^{-1}$). A classical electro-optical set up was used for the measurement of switching current, response time and apparent tilt angle.

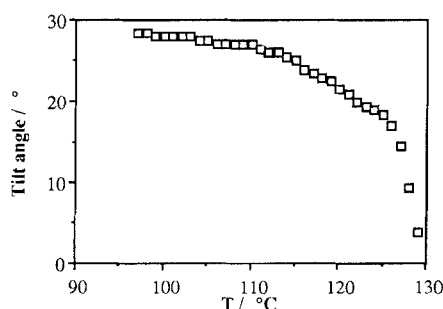


Figure 8. Apparent tilt angle versus temperature ($E = \pm 2 \text{ V } \mu\text{m}^{-1}$; $\nu = 0.2 \text{ Hz}$).

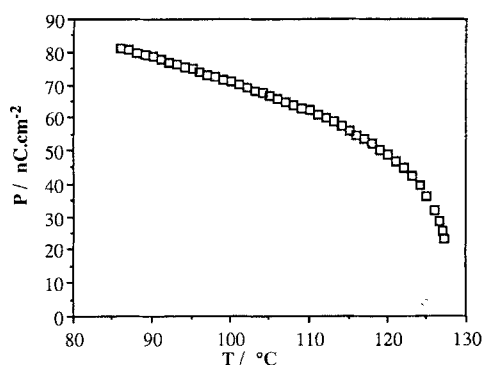


Figure 9. Spontaneous polarization versus temperature ($E = \pm 2 \text{ V } \mu\text{m}^{-1}$; $\nu = 15 \text{ Hz}$).

(i) The apparent tilt angle θ of the molecules from the normal to the smectic layers was measured from the difference between the extinction positions between crossed polarizer and analyser under an AC field ($\pm 2 \text{ V } \mu\text{m}^{-1}$) and at very low frequency (0.2 Hz). The field was sufficient to induce the phase transition from all $S_{C\alpha}^*$, S_{CFI}^* , S_{CA}^* phases to the S_C^* phase (see figure 8).

(ii) The spontaneous polarization measurements (see figure 9) were also performed under an AC field at saturation ($E = \pm 2 \text{ V } \mu\text{m}^{-1}$). In both cases, no anomaly could be detected on the $\theta(T)$ and the $P(T)$ curves at the phase transitions.

(iii) On the contrary, the measurement of the polarization versus field shows significant differences from one phase to the other. The S_{CA}^* phase requires a relatively high field to accomplish transition to the ferroelectric phases, and there is a threshold field (see figure 10). The threshold diminishes with temperature (see figure 11). In the S_{CFI}^* and S_{CF2}^* phases the behaviour is similar (which supports our suggestion that both phases are of the same nature): at low field a step is reached approximately at $P/2$; this step seems to be characteristic of these phases (see figure 12). Finally, in the S_C^* phase, saturation is reached with a field as low as $1 \text{ V } \mu\text{m}^{-1}$ (see figure 13).

6. Pitch measurements

We have used the dodecyloxy derivative for helical pitch measurements. As previously described [18], we use prismatic cells with a weak edge angle (< 0.25 degree) oriented in the Grandjean–Cano texture; the required orientation is complanar (pseudo-homeotropic). A good orientation is easily obtained in the S_C^* phase leading to the observation of a large number of equal width Grandjean–Cano steps, thus allowing

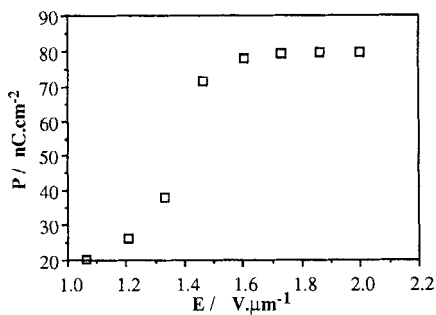


Figure 10. Polarization versus field at 88°C (S_{CA}^* phase; $\nu = 15$ Hz).

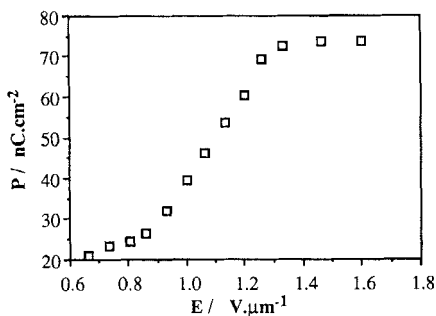


Figure 11. Polarization versus field at 98°C (S_{CA}^* phase; $\nu = 15$ Hz).

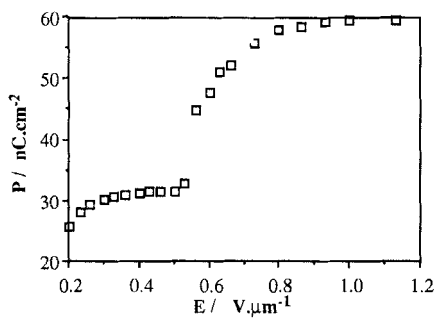


Figure 12. Polarization versus field at 110°C (S_{CFI}^* phase; $\nu = 15$ Hz).

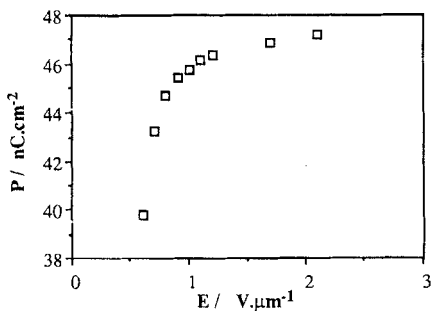


Figure 13. Polarization versus field at 120°C (S_C^* phase; $\nu = 15$ Hz).

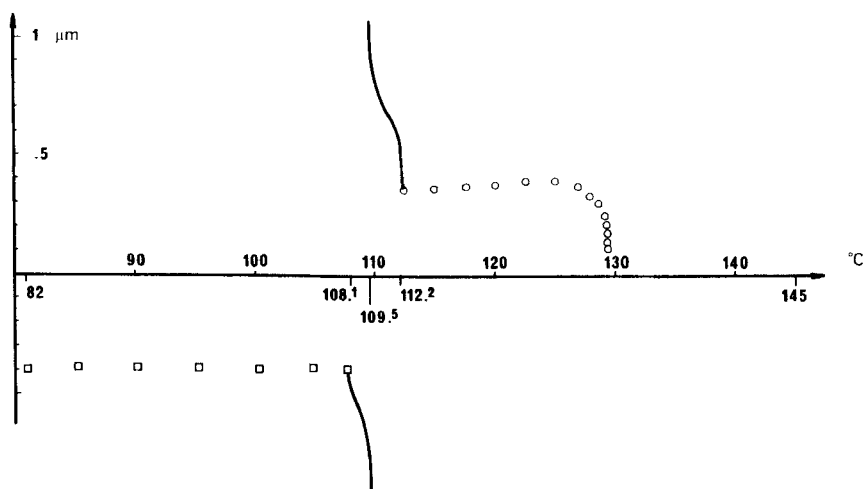


Figure 14. Helical pitch versus temperature in the S_C^* phase (open circles), $S_{C_{FI}}^*$ phase (full line) and $S_{C_A}^*$ phase (open squares).

an accurate measurement of the pitch and of its temperature dependence. On the contrary the quality of the orientation is rather poor for the $S_{C_A}^*$ phase, with only a few steps available (2 to 5).

The selective reflection of the light occurring for the S_C^* and $S_{C_A}^*$ phases allows a check on the measured pitch values: we have especially verified that the Grandjean steps are actually related to the full pitch in the S_C^* phase and to half the pitch in the $S_{C_A}^*$ phase. Moreover, the direction of rotation of the helix can be determined by analysing the direction of the circularly polarized reflected light and/or the sign of the rotatory power. In the $S_{C_{FI}}^*$ phases, no Grandjean–Cano steps could be obtained and we cannot provide any precise value of the pitch for these phases. Thus we provide only a qualitative description of the variations of the helix. These have been established from complanar flat droplets [18] in which one can observe: (i) equal thickness fringes, roughly parallel to the edge of the drop, which tighten when the pitch decreases and move apart when the pitch increases and (ii) disordered Grandjean–Cano threads which cross the sample more or less rapidly, accounting for a more or less important temperature dependence of the twist. Altogether the results are reported in figure 14.

At low temperature in the S_C^* phase, the very short pitch ($p = 0.355 \mu\text{m}$ at 112.3°C) corresponds to selective reflection of green light (normal reflection, with $\lambda = np = 0.55 \mu\text{m}$); the pitch slowly increases with temperature up to $0.39 \mu\text{m}$ at 125°C , the corresponding colour being yellow green. Then the pitch decreases between 125 and 129°C : the colour changes progressively from yellow to green, blue and violet. Finally a sudden steep drop in the pitch occurs at about 129.2°C – 129.4° from $0.27 \mu\text{m}$ to less than $0.135 \mu\text{m}$, with a rapid change of the colours over a second complete visible spectrum; these last reflections are related to the pitch by $\lambda = 2np$ and are the so-called ‘full pitch reflections’ for very short values of the pitch. This last sudden step is a commonly observed signature of a weakly first order or second order S_C^* – S_A transition. We note that we cannot distinguish the $S_{C_x}^*$ phase in these pitch measurement experiments. In addition the sense of the rotary power and the sense of the circularly polarized reflected light indicate that the helix is right handed for the S_C^* phase of the *R* enantiomer.

In the S_{CA}^* phase, the pitch is also very short and remains quasi-constant: $p = 0.40 \mu\text{m}$ (orange reflection) at 85°C , $0.39 \mu\text{m}$ (orange yellow reflection) at 107.6°C ; the sense of the helix is left handed, opposite to that observed for the S_C^* phase. In fact the reversal of the helix occurs somewhere in the domain corresponding to the S_{CF1}^* and S_{CF2}^* phases. The twist ($1/p$) varies steeply on both sides of the ferroelectric domain with rapid variations of the reflected colours (see full lines in figure 14); then the variation of the twist slows down and seems to be progressive, and finally the pitch diverges at the reversal. The two different S_{CF}^* phases cannot actually be distinguished, but we suggest that this reversal could correspond to the phase change. These difficulties are partly due to the large hysteresis effects observed during these experiments: on cooling the $S_{CF(1+2)}^*$ phase extends from 112.2°C to 108.5°C , the pitch switching at about 109.5°C ; on heating the limits of the ferroelectric domain are 110.8°C and 115.2°C , the pitch switching at 114°C . These variations in the S_{CF}^* domain do not agree with the following relation which supposes a periodic structure with three layers, one tilted in a direction opposite to the other two, as proposed by Takezoe *et al.* [19]:

$$\frac{1}{ps_{CF}^*} = \frac{1}{3} \left(\frac{2}{ps_{CA}^*} + \frac{1}{ps_C^*} \right).$$

According to this, one expects a constant twist in the S_{CF}^* phase, since the twist remains almost constant in both the S_{CA}^* and S_C^* phases.

7. Conclusions

The new chiral series with the thiobenzoate core described in this paper displays a complex smectic mesomorphism: $S_{CA}^* S_{CF1}^* S_C^* S_{CA}^* S_A$. These compounds have allowed an improvement in the knowledge of these different phases. In particular DSC and optical observations indicate that two S_{CF}^* phases can exist between the S_C^* and S_{CA}^* phases. Strong odd–even effects are observed not only with the chiral chain length, but also with the achiral chain length. A reentrant S_C phase is obtained in a pure compound. The pitch measurements show that the pitch is short in the S_C^* and S_{CA}^* phases, but their twist sense is inverted. Within the S_{CF}^* domain the pitch varies greatly with change in the sense of the twist. The electro-optical measurements show a different behaviour for all the helical smectic phases as a function of field. Especially we observe a middle plateau in the polarization at low field in the S_{CF}^* state. The exact structure of these ferroelectric smectic phases (as well as that of the S_{CA}^* phase) needs clarification.

References

- [1] CHANDANI, A. D. L., OUCHI, Y., TAKEZOE, H., FUKUDA, A., TERASHIMA, K., FURUKAWA, K., and KISHI, A., 1989, *Jap. J. appl. Phys.*, **28**, 1261.
- [2] YAMAWAKI, M., YAMADA, Y., MORI, N., HAYASHI, H., SUZUKI, Y., NEGI, Y. S., KAWAMURA, T., and ISHIBASHI, H., 1989, *Proceedings of 9th International Display Res. Conference*, **3**, 26.
- [3] YAMADA, Y., YAMAMOTO, N., MORI, K., NAKAMURA, K., HAGIWARA, K., SUZUKI, Y., KAWAMURA, I., ORIHARA, H., and ISHIBASHI, Y., 1990, *Jap. J. appl. Phys.*, **29**, 1757.
- [4] JOHNO, M., CHANDANI, A. D. L., LEE, J., OUCHI, Y., TAKEZOE, H., FUKUDA, A., ITOH, K., and KITAZUME, T., 1989, *Proc. Jap. Display*, p. 22.
- [5] SUZUKI, Y., HAGIMURA, T., KAWAMURA, I., OKAMURA, N., KITAZUME, T., KAKIMOTO, M., IMAI, Y., OUCHI, Y., TAKEZOE, H., and FUKUDA, A., 1989, *Liq. Crystals*, **6**, 167.
- [6] LI, J., TAKEZOE, H., and FUKUDA, A., 1991, *Jap. J. appl. Phys.*, **30**, 532.
- [7] INUI, S., KAWANO, S., IWANE, H., TAKANISHI, Y., HIRAOKA, K., OUCHI, Y., TAKEZOE, H., and FUKUDA, A., 1990, *Jap. J. appl. Phys.*, **29**, 987.
- [8] IKEDA, A., TAKANISHI, Y., TAKEZOE, H., and FUKUDA, A., 1993, *Jap. J. appl. Phys.*, **32**, 97.

- [9] GOODBY, J. W., PATEL, J. S., and CHIN, E., 1992, *J. mater. Chem.*, **2**, 197.
- [10] GOODBY, J. W., and CHIN, E., 1988, *Liq. Crystals*, **3**, 1245.
- [11] HEPPKE, G., KLEINEBERG, P., LOTZSCH, D., MERY, S., and SHASHIDAR, R., 1993, *Molec. Crystals liq. Crystals*, **231**, 257.
- [12] LEVELUT, A. M., GERMAIN, C., KELLER, P., LIEBERT, L., and BILLARD, J., 1993, *J. Phys., Paris*, **44**, 623.
- [13] GALERNE, Y., and LIEBERT, L., 1990, *Phys. Rev. Lett.*, **64**, 906.
- [14] GALERNE, Y., and LIEBERT, L., 1991, *Phys. Rev. Lett.*, **66**, 2891.
- [15] TAKEZOE, H., FUKUDA, A., IKEDA, A., TAKANISHI, Y., UMEMOTO, T., WATANABE, J., IWANE, H., HARA, M., and ITOH, K., 1991, *Ferroelectrics*, **122**, 167.
- [16] HAMELIN, P., LEVELUT, A. M., MARTINOT-LARGARDE, P., GERMAIN, C., and LIEBERT, L., 1993, *J. Phys. II, France*, **3**, 681.
- [17] NISHIYAMA, I., YOSHIZAWA, A., FUKUMASA, M., and HIRAI, T., 1988, *Jap. J. appl. Phys.*, **28**, L-2248.
- [18] BRUNET, M., and ISAERT, N., 1988, *Ferroelectrics*, **84**, 25.
- [19] TAKEZOE, H., LEE, J., OUCHI, Y., and FUKUDA, A., 1991, *Molec. Crystals liq. Crystals*, **202**, 85.